

# Time dependence of multiply scattered diffuse ultrasound in polycrystalline media

Joseph A. Turner and Richard L. Weaver

Department of Theoretical and Applied Mechanics, 216 Talbot Laboratory, 104 South Wright Street, University of Illinois at Urbana-Champaign, Urbana, Illinois 61801

(Received 27 June 1994; accepted for publication 2 January 1995)

Time domain results are presented for the multiply scattered longitudinal intensity backscattered from a polycrystalline medium. The results are solutions to the ultrasonic radiative transfer equation (URTE), the derivation of which is based upon radiative transfer theory. Unlike steady-state solutions obtained previously, time domain solutions will more closely correspond to experiments that use tone burst sources. This paper is concerned with the time dependence of the backscattered longitudinal intensity from a polycrystalline medium excited by a normally incident longitudinal wave idealized as an impulsive deposition of energy. It is shown that multiple scattering effects become significant at times on the order of a mean free time or less. It is anticipated that this work may be applicable to microstructural characterization of polycrystalline, geophysical and other random media in which multiple scattering effects are important.

PACS numbers: 43.20.Gp, 43.20.Bi, 43.35.Cg

## INTRODUCTION

Microstructural characterization of polycrystalline materials using diffuse or incoherent ultrasonic fields is becoming a powerful microstructural characterization tool.<sup>1-6</sup> Experiments involving diffuse fields, although requiring extensive spatial averaging, offer greater flexibility for *in-situ* measurements and require less stringent geometric conditions (e.g., parallel surfaces) than conventional coherent field measurements.<sup>7-11</sup> Researchers have thus far been successful in characterizing polycrystalline materials through measurements of the backscattered intensity. Some of the models developed to predict the backscattered intensity for polycrystalline materials have been based on single scattering assumptions which are valid for weakly scattering materials, early times, or instances when narrowly focused beams are used.<sup>4-6</sup> Other models for the diffuse intensities are based on the diffusive limit in which the ultrasonic energy has scattered sufficiently many times that it can be modeled using a diffusion equation.<sup>12,13</sup> In many cases, however, the intermediate multiple scattering range is important. Unlike the singly scattered fields, the multiply scattered fields are sensitive to the angular dependence of the scattering amplitudes and to absorption as well as to scattering.

A method was recently presented to model the multiply scattered diffuse intensity of ultrasound in polycrystalline media.<sup>13-15</sup> This model includes all multiple scattering effects and thus covers the entire multiple scattering range from single scattering to the diffusive limit. It is based on radiative transfer theory<sup>16-19</sup> in which an ultrasonic radiative transfer equation (URTE) is derived. Thus far only steady-state solutions of the URTE have been presented<sup>14,15</sup> which, ordinarily, do not reflect typical experiments that are currently performed with diffuse intensity. Such experiments are usually done in the time domain using short tone bursts. Time domain solutions to the URTE were briefly discussed by Turner and Weaver,<sup>14</sup> but none were presented. In this

paper we discuss these temporal solutions due to a normally incident longitudinal wave idealized as an impulsive deposition of longitudinal energy. It is shown that the full multiply scattered field exhibits behavior dramatically different than the singly scattered field, and that the effects of multiple scattering may be significant at times on the order of a mean free time or less.

The ultrasonic radiative transfer equation is presented and discussed in the next section. Section II contains the derivation of closed form solutions for the singly scattered intensities. In Sec. III, we present numerical solutions for the complete backscattered longitudinal intensity as a function of time for the case of polycrystalline iron.

## I. ULTRASONIC RADIATIVE TRANSFER THEORY

The ultrasonic radiative transfer equation (URTE) has been derived for a polycrystalline medium through an examination of ensemble averaged responses of the elastic wave equation by the use of the Bethe-Salpeter equation.<sup>13,15</sup> It is expected to be valid within the limit of its primary assumption that the material heterogeneity is weak. This criterion is satisfied by a large number of materials of common interest. The URTE governs the propagation of diffuse intensities and includes all multiple scattering effects.

The steady state solutions presented previously<sup>14,15</sup> exhibit many of the features expected for a multiple scattering model. In the limit of high absorption, the solution reduces to a single scattering solution. In the opposite limit, deep within the medium and after the intensities have scattered many times, the solution approaches a diffusive limit with the expected equipartitioning of energy.<sup>13,20</sup> Steady-state solutions cannot, however, model the time domain behavior observed in current experimental work. This paper is concerned, therefore, with the extension of the previously developed theory to the case of time varying intensities. In this section the

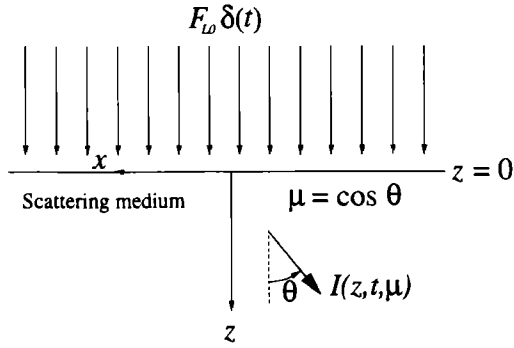


FIG. 1. Geometry of the problem.

ultrasonic radiative transfer equation is presented with the time dependence retained.

It should be noted that this problem contains two distinct time scales which are Fourier transformed to two distinct frequencies. The *inner* frequency,  $\omega$ , defines the excitation frequency which governs the elastic wave equation used for the derivation of the URTE. This frequency is typically of order several MHz. The *outer* frequency,  $\Omega$ , typically of the order of several hundred kHz, defines the frequency which governs the much slower temporal evolution of the diffuse intensities governed by the URTE. In the assumed limit that the material heterogeneities are weak, these time scales are widely separated and the distinction between  $\omega$  and  $\Omega$  is legitimate.

The geometry of the problem to be discussed is shown in Fig. 1. The medium is invariant in the  $x$  and  $y$  directions and is semi-infinite in the  $z$  direction. A normally incident longitudinal wave with incident flux  $F_{L0}$  and delta function time dependence (as discerned on the outer scale) is used as the excitation input. On the inner time scale, one may think of this input as a short tone burst with center frequency  $\omega$ . With this axisymmetric incident field the intensity in the medium varies as a function of depth, time, and direction of propagation. This direction is given by  $\mu$ , the cosine of the angle between the direction of the intensity of interest and the  $z$  axis. The intensity at  $\mu < 0$  is in the upward direction out of the scattering medium and the intensity at  $\mu > 0$  is in the downward direction, into the scattering medium.

As discussed previously,<sup>14,15</sup> the URTE for this problem may be written

$$\begin{aligned} \mu \frac{\partial \mathbf{I}(\tau, \xi, \mu)}{\partial \tau} + \tilde{\mathbf{c}}^{-1} \frac{\partial \mathbf{I}(\tau, \xi, \mu)}{\partial \xi} + (\tilde{\mathbf{k}} + \tilde{\mathbf{v}}) \mathbf{I}(\tau, \xi, \mu) \\ = \frac{1}{2\kappa_T} \int_{-1}^{+1} \mathbf{P}(\mu; \mu') \mathbf{I}(\tau, \xi, \mu') d\mu' \\ + \mathbf{S}_L(\mu, \mu_0) e^{-\tilde{\alpha}_L \tau / \mu_0} \delta(\xi - c_T \tau / c_L \mu_0), \end{aligned} \quad (1)$$

where the Stokes vector,  $\mathbf{I}$ , contains the five elastic Stokes parameters, one longitudinal,  $I_L$ , and four shear,  $I_{SV}$ ,  $I_{SH}$ ,  $U$ , and  $V$  which completely characterize the diffuse intensity. The total intensity is obtained by including the incident wave also.

The incident direction  $\mu_0$  is  $+1.0$ . The matrices  $\tilde{\mathbf{c}}$ ,  $\tilde{\mathbf{k}}$ , and  $\tilde{\mathbf{v}}$  define the dimensionless wave speed, scattering, and absorption matrices which are given by

$$\begin{aligned} \tilde{\mathbf{c}} = \begin{bmatrix} \frac{c_L}{c_T} & 0 & 0 & 0 & 0 \\ 0 & 1 & 0 & 0 & 0 \\ 0 & 0 & 1 & 0 & 0 \\ 0 & 0 & 0 & 1 & 0 \\ 0 & 0 & 0 & 0 & 1 \end{bmatrix}, \quad \tilde{\mathbf{k}} = \begin{bmatrix} \frac{\kappa_L}{\kappa_T} & 0 & 0 & 0 & 0 \\ 0 & 1 & 0 & 0 & 0 \\ 0 & 0 & 1 & 0 & 0 \\ 0 & 0 & 0 & 1 & 0 \\ 0 & 0 & 0 & 0 & 1 \end{bmatrix}, \\ \tilde{\mathbf{v}} = \frac{1}{\kappa_T} \begin{bmatrix} \nu_L & 0 & 0 & 0 & 0 \\ 0 & \nu_T & 0 & 0 & 0 \\ 0 & 0 & \nu_T & 0 & 0 \\ 0 & 0 & 0 & \nu_T & 0 \\ 0 & 0 & 0 & 0 & \nu_T \end{bmatrix}, \end{aligned} \quad (2)$$

where  $c_L$  and  $c_T$ ,  $\kappa_L$  and  $\kappa_T$ ,  $\nu_L$  and  $\nu_T$  are the wave speeds, intensity scattering attenuations, and intensity absorption attenuations for the longitudinal ( $L$ ) and transverse ( $T$ ) modes. The dimensionless total attenuations,  $\tilde{\sigma}_L = (\kappa_L + \nu_L) / \kappa_T$  and  $\tilde{\sigma}_T = 1 + \nu_T / \kappa_T$ , include both scattering and absorption. The dimensionless depth,  $\tau = \kappa_T z$ , is measured in units of inverse shear intensity attenuation, while the dimensionless time,  $\xi = c_T \kappa_T t$ , is measured in units of shear intensity mean-free time. The Mueller matrix,  $\mathbf{P}$ , governs the scattering between each of the Stokes parameters. It contains combinations of inner products of the covariance of elastic moduli fluctuations and wave vectors.  $\mathbf{P}$  is also a function of the spatial Fourier transform of the two-point correlation function of the material properties.<sup>13,15</sup> This matrix is parametrically dependent upon the inner frequency,  $\omega$ , and is directly related to  $\tilde{\mathbf{k}}$ . It has been derived for polycrystalline aggregates with cubic<sup>15</sup> and hexagonal crystallites.<sup>21</sup>

The diffuse intensity has a source,  $\mathbf{S}_L$ , due to a normally incident ( $\mu_0 = +1$ ) longitudinal wave. It is given by

$$\mathbf{S}_L(\mu, \mu_0 = +1) = \begin{Bmatrix} S_{LL} \\ S_{LT} \end{Bmatrix} = \frac{F_{L0}}{2\kappa_T} \begin{Bmatrix} P_{11}(\mu; \mu_0 = +1) \\ P_{21}(\mu; \mu_0 = +1) \\ P_{31}(\mu; \mu_0 = +1) \\ P_{41}(\mu; \mu_0 = +1) \\ 0 \end{Bmatrix}, \quad (3)$$

and includes a contribution  $S_{LL}$  which is the singly scattered longitudinal to longitudinal part, and a contribution  $S_{LT}$  which is the remaining four-component vector containing the singly scattered longitudinal to shear parts. The delta function time dependence in the source term in Eq. (1) has a time shift to satisfy causality within the medium.

A Fourier transform pair may be defined which governs the transform between dimensionless outer time,  $\xi$ , and dimensionless outer frequency,  $\Omega$ . This transform pair is

$$\begin{aligned} \tilde{\mathbf{I}}(\tau, \Omega, \mu) &= \int_{-\infty}^{+\infty} \mathbf{I}(\tau, \xi, \mu) e^{-i\Omega \xi} d\xi, \\ \mathbf{I}(\tau, \xi, \mu) &= \frac{1}{2\pi} \int_{-\infty}^{+\infty} \tilde{\mathbf{I}}(\tau, \Omega, \mu) e^{i\Omega \xi} d\Omega. \end{aligned} \quad (4)$$

With this transform definition, Eq. (1) becomes

$$\begin{aligned} & \mu \frac{\partial \tilde{\mathbf{I}}(\tau, \Omega, \mu)}{\partial \tau} + (\tilde{\kappa} + \tilde{\nu} + i\Omega \tilde{\mathbf{C}}^{-1}) \tilde{\mathbf{I}}(\tau, \Omega, \mu) \\ &= \frac{1}{2\kappa_T} \int_{-1}^{+1} \mathbf{P}(\mu; \mu') \tilde{\mathbf{I}}(\tau, \Omega, \mu') d\mu' \\ &+ S_L(\mu, \mu_0 = +1) e^{-\tilde{\sigma}_L \tau / \mu_0 - i\Omega c_T \tau / c_L \mu_0}. \end{aligned} \quad (5)$$

We discuss solutions of this equation in the next two sections. Solutions to other types of incident time histories may be found by convolution.

## II. SINGLY SCATTERED SOLUTIONS

A single scattering assumption is often used with good success for materials with weak scattering, for early times, or for experiments involving focused transducers.<sup>4-6</sup> The implication is that the intensity scatters only once before exiting the medium. The independent scatterer model<sup>4</sup> is one such model. The singly scattered intensity, using radiative transfer theory, is the solution to Eq. (5) with the integral term removed. This solution has been developed for the steady-state case<sup>14,18</sup> in which  $\Omega=0$ . Here we generalize that solution to the case  $\Omega \neq 0$  and obtain the singly scattered solution as a function of the outer frequency due to an impulsive deposition of normally incident longitudinal energy. This solution is then analytically transformed back to the time domain and shown to be equivalent to the independent scatterer model.<sup>4,5</sup>

The singly scattered longitudinal intensity in the outer frequency domain in the upward ( $\mu < 0$ ) and downward ( $\mu > 0$ ) directions is the solution of Eq. (5) without the integral term<sup>14,15</sup>

$$\begin{aligned} \tilde{I}_L(\tau, \Omega, \mu < 0) &= \frac{S_{LL} e^{-\tilde{\sigma}_L \tau / \mu_0 - i\Omega c_T \tau / \mu_0 c_L}}{-\mu(1/\mu_0 - 1/\mu)(\tilde{\sigma}_L + i\Omega c_T / c_L)}, \\ \tilde{I}_L(\tau, \Omega, \mu > 0) &= \frac{S_{LL}(e^{-\tilde{\sigma}_L \tau / \mu - i\Omega c_T \tau / c_L \mu} - e^{-\tilde{\sigma}_L \tau / \mu_0 - i\Omega c_T \tau / c_L \mu_0})}{\mu(1/\mu_0 - 1/\mu)(\tilde{\sigma}_L + i\Omega c_T / c_L)}. \end{aligned} \quad (6)$$

The transverse intensities are given by

$$\begin{aligned} \tilde{\mathbf{I}}_T(\tau, \Omega, \mu < 0) &= \frac{S_{LT} e^{-\tilde{\sigma}_L \tau / \mu_0 - i\Omega c_T \tau / c_L \mu_0}}{-\mu[\tilde{\sigma}_L / \mu_0 - \tilde{\sigma}_T / \mu + i\Omega(c_T / c_L \mu_0 - 1/\mu)]}, \\ \tilde{\mathbf{I}}_T(\tau, \Omega, \mu > 0) &= \frac{S_{LT}(e^{-\tilde{\sigma}_T \tau / \mu - i\Omega \tau / \mu} - e^{-\tilde{\sigma}_L \tau / \mu_0 - i\Omega c_T \tau / c_L \mu_0})}{\mu[\tilde{\sigma}_L / \mu_0 - \tilde{\sigma}_T / \mu + i\Omega(c_T / c_L \mu_0 - 1/\mu)]}. \end{aligned} \quad (7)$$

The inverse transforms may be obtained by straightforward application of the Cauchy residue theorem. The resulting time dependent singly scattered intensities are

$$\begin{aligned} I_L(\tau, \xi, \mu < 0) &= \frac{S_{LL} c_L e^{-\tilde{\sigma}_L c_L \xi / c_T}}{-\mu c_T (1/\mu_0 - 1/\mu)} H(\xi - c_T \tau / c_L \mu_0), \\ I_L(\tau, \xi, \mu > 0) &= \frac{S_{LL} c_L e^{-\tilde{\sigma}_L c_L \xi / c_T}}{\mu c_T (1/\mu_0 - 1/\mu)} [H(\xi - c_T \tau / c_L \mu) \\ &- H(\xi - c_T \tau / c_L \mu_0)], \end{aligned} \quad (8)$$

and

$$\begin{aligned} I_T(\tau, \xi, \mu < 0) &= \frac{S_{LT} e^{-\tau \tilde{\sigma}_L / \mu_0} e^{-\zeta_{LT}(\xi - c_T \tau / c_L \mu_0)}}{-\mu(c_T / c_L \mu_0 - 1/\mu)} \\ &\times H(\xi - c_T \tau / c_L \mu_0), \\ I_T(\tau, \xi, \mu > 0) &= \frac{S_{LT} e^{-\tau \tilde{\sigma}_L / \mu_0} e^{-\zeta_{LT}(\xi - c_T \tau / c_L \mu_0)}}{\mu(c_T / c_L \mu_0 - 1/\mu)} \\ &\times [H(\xi - \tau / \mu_0) - H(\xi - c_T \tau / c_L \mu_0)], \end{aligned} \quad (9)$$

where we have defined

$$\zeta_{LT} = \frac{(\tilde{\sigma}_L / \mu_0 - \tilde{\sigma}_T / \mu)}{(c_T / c_L \mu_0 - 1/\mu)} \quad (10)$$

for convenience. This quantity,  $\zeta_{LT}$ , is the pole of Eqs. (7) divided by  $i = \sqrt{-1}$ . It governs the temporal decay of the mode converted ray and is equal to the total travel path attenuation divided by the inverse of the total wave speed along the travel path. Thus  $\zeta_{LT}$  is related to the inverse amount of time a mode converted ray takes to scatter. Here,  $H(x)$  is the Heaviside step function which is equal to unity for  $x > 0$ .

Using Eq. (8) we can write the solution to the singly scattered longitudinal intensity in the backscatter ( $\mu = -1$ ) direction at the surface of the material ( $\tau = 0$ ) as,

$$\begin{aligned} I_L(\tau = 0, \xi, \mu = -1) &= \frac{c_L}{4c_T \kappa_T} P_{11}(\mu = -1; \mu_0 = +1) e^{-\tilde{\sigma}_L c_L \xi / c_T} H(\xi), \end{aligned} \quad (11)$$

where the definition of  $S_{LL}$  given in Eq. (3) has been used. If the definition of  $P_{11}$  for cubic crystallites is used,<sup>15</sup> evaluated at  $\mu_0 = +1$  and  $\mu = -1$  we find that

$$\begin{aligned} I_L(\tau = 0, \xi, \mu = -1) &= \frac{c_L}{4c_T \kappa_T} \frac{32\beta v^2}{525\rho^2 c_L^4} \frac{x_L^4}{[1 + (2x_L)^2]^2} e^{-\tilde{\sigma}_L c_L \xi / c_T} H(\xi), \end{aligned} \quad (12)$$

where  $v = C_{11} - C_{12} - 2C_{44}$  is the crystallite anisotropy and  $x_L = \omega / c_L \beta$  is a dimensionless measure of inner frequency. An exponential two-point correlation function of the form  $e^{-\beta r}$  has also been assumed where  $\beta$  is an inverse measure of the length scale. The amplitude of the backscattered longitudinal intensity has the same frequency, time, and material dependence as the backscattered power given by Rose<sup>5</sup> using independent scatterer theory. Thus the independent scatterer model may be considered to be a limiting case of the URTE.

## III. MULTIPLY SCATTERED SOLUTIONS

Solutions to the entire URTE given in Eq. (5) must be obtained numerically for a given excitation frequency,  $\omega$ .<sup>14</sup> The discrete ordinates method<sup>14,16,18</sup> was used to solve the URTE in outer frequency space. The resulting intensities were then numerically transformed back to the outer time domain.

The Mueller matrix,  $\mathbf{P}$ , was obtained by assuming an exponential two-point correlation function as discussed above and elsewhere.<sup>13,15</sup> Using parameters corresponding to polycrystalline iron, the dimensionless crystallite anisotropy,

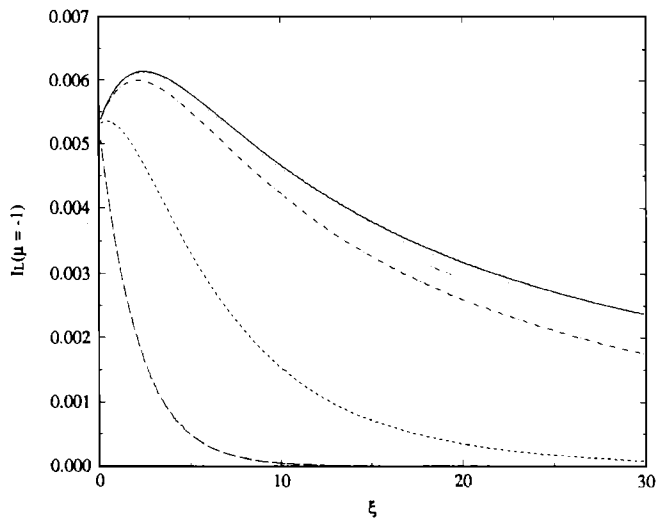


FIG. 2. Backscattered ( $\mu = -1$ ) longitudinal intensity versus dimensionless time at dimensionless inner frequency  $x_T = 0.5$  for different absorption rates: No absorption (solid line),  $\tilde{\nu}_T = 0.001$  (dotted),  $\tilde{\nu}_T = 0.01$  (dot dash),  $\tilde{\nu}_T = 0.111$  (small dash). The singly scattered solution without absorption [Eq. (8)] is shown by the large dashes.

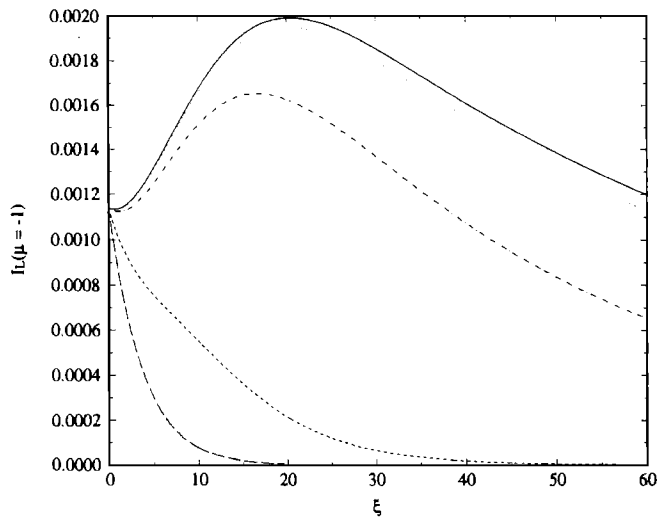


FIG. 3. Backscattered ( $\mu = -1$ ) longitudinal intensity versus dimensionless time at dimensionless inner frequency  $x_T = 3.0$  for different absorption rates: No absorption (solid line),  $\tilde{\nu}_T = 0.001$  (dotted),  $\tilde{\nu}_T = 0.01$  (dot dash),  $\tilde{\nu}_T = 0.111$  (small dash). The singly scattered solution without absorption [Eq. (8)] is shown by the large dashes.

$v/\rho c_T^2 = -1.66$  and  $c_L/c_T = 1.827$ . Results for the multiply scattered longitudinal intensity in the backscatter direction ( $\mu = -1$ ) are shown in Fig. 2 as a function of dimensionless time,  $\xi = c_T \kappa_T t$  at a dimensionless inner frequency of  $x_T = \omega/c_T \beta = 0.5$ . Each curve was calculated at a different absorption rate using the dimensionless absorption defined as the ratio of the absorption attenuation to the scattering attenuation,  $\tilde{\nu}_T = \nu_T/\kappa_T$ . The absorption per wavelength for the different modes was assumed equal which implies that  $c_L \nu_L = c_T \nu_T$ . The absorption would normally be frequency dependent, but for simplicity, it is given here as a fraction of the scattering attenuation.

The results show that the multiply scattered intensity is equal to the singly scattered intensity at early times as expected. After only a few mean-free times, however, the multiply scattered solution has deviated sharply from the singly scattered solution. The multiply backscattered intensity quickly rises to a peak and then begins an asymptotic decay. As the absorption is increased, the multiply scattered solution approaches the absorptive singly scattered solution as expected. In this case, multiple scattering effects are quickly dampened out.

The peak in these solutions was rather unexpected. The energy that arrives before this peak has a large single scattering component. After the peak, however, the signal contains almost no singly scattered energy. The arrival time of the peak is also a function of the wave speed ratio, listening direction, and inner frequency. In fact, as the wave speeds become less disparate this peak arrives earlier in time and can become nonexistent. In this case, the intensity begins at its peak value and then decays. Thus this peak may be due to the attenuation ratio which allows the incident longitudinal energy to penetrate deeper than the shear energy which delays the return of that energy to the surface. The unexpected peak and additional structure of the multiply scattered solution underscore the added microstructural information avail-

able in the multiply scattered fields compared with the singly scattered fields.

Figure 3 shows the backscattered intensity for iron at a higher dimensionless excitation frequency,  $x_T = 3.0$ . The results are similar, except for the location of the peak in the multiply scattered solution. The peak now occurs at about 21 shear mean-free times for zero absorption after almost all of the singly scattered energy has decayed. The shift of this peak is due to the directional dependence of the scattering. The greater amount of forward scattering that occurs at the higher frequency,<sup>15</sup> delays the time for much of the energy to be multiply scattered into the backward direction. This directionality of the scattering also amplifies the effects of absorption. The high frequency results with absorption deviate more quickly from the zero absorption solution than the low frequency results of Fig. 2.

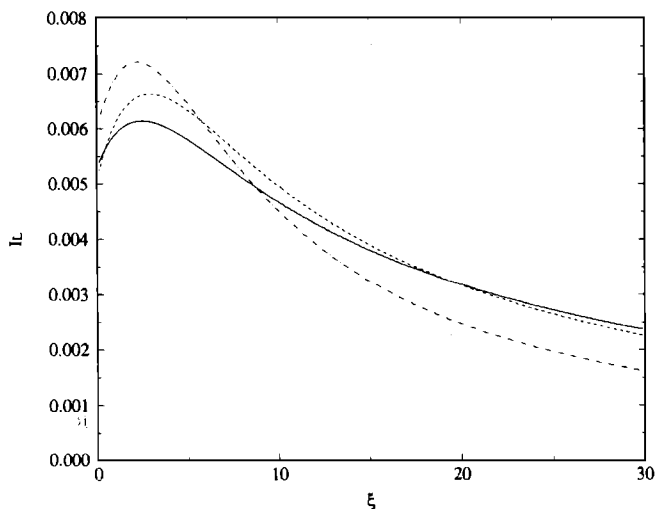


FIG. 4. Upward longitudinal intensity versus dimensionless time at dimensionless inner frequency  $x_T = 0.5$  in three different directions:  $0^\circ$  (solid line),  $48.5^\circ$  (dashed), and  $76.2^\circ$  (dot-dash) from vertical.

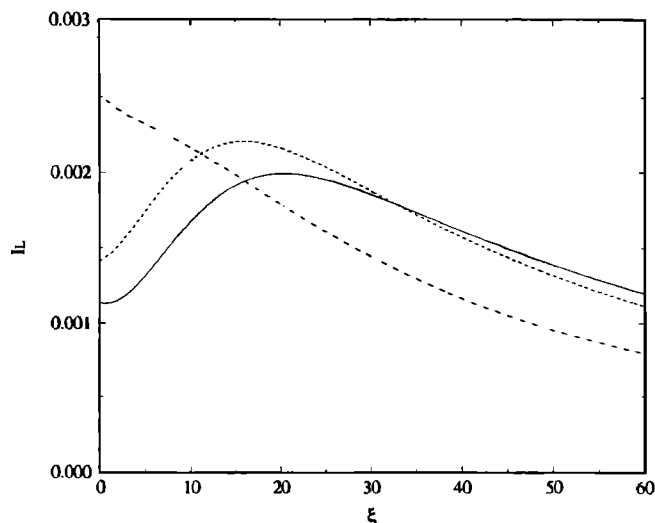


FIG. 5. Upward longitudinal intensity versus dimensionless time at dimensionless inner frequency  $x_T=3.0$  in three different directions:  $0^\circ$  (solid line),  $48.5^\circ$  (dashed), and  $76.2^\circ$  (dot-dash) from vertical.

The results shown in Figs. 2 and 3 have similar trends. They begin at the single scattering solution, rise to some maximum, and then reach an asymptotically decaying limit. This late time behavior is expected to correspond to the diffusion limit where the energy is nearly isotropic and equipartitioned.<sup>13,20</sup> The approach to the diffusive limit and the validity of the diffusion approximation are topics for a future communication.

The angular dependence of the backscatter peak is shown in Figs. 4 and 5 for  $x_T=0.5$  and  $x_T=3.0$ , respectively. The results are the upward longitudinal intensity in three directions:  $0^\circ$ ,  $48.5^\circ$ , and  $76.2^\circ$  from vertical. The low-frequency results display the general isotropic scattering nature expected. The energy peaks do not arrive at precisely identical times, but the peaks are fairly closely spaced in time. At the higher frequency, shown in Fig. 5, these peaks are distinctly separated. The separation between the peaks alludes to the time for the forward scattered energy to return to the backscatter direction. The arrival time of these peaks as a function of direction provides insight into the directional tendency of the scattering functions which governs the multiple scattering process.

The time for the multiply scattered intensity to be significant in comparison with the singly scattered intensity can also be examined. After a certain amount of time, the multiple scattering effects will be of primary importance. These results can be put into dimensional units for greater clarity. Table I contains the time for the multiply scattered intensity to be twice that of the singly scattered. Two materials are considered: Iron which scatters strongly and aluminum

TABLE I. Time for the multiply scattered longitudinal intensity to be twice the singly scattered intensity for iron and aluminum at two frequencies with  $\beta=10/\text{mm}$ .

$f(\text{MHz})$	Fe	Al
2.5	$8.65 \mu\text{s}$	$155 \mu\text{s}$
15	0.241	5.58

TABLE II. Mean free times ( $1/c\kappa$ ) for iron and aluminum for both propagation modes.

$f(\text{MHz})$		Mean free times ( $1/c\kappa$ )	
		Fe	Al
2.5	<i>L</i>	$15.1 \mu\text{s}$	$309 \mu\text{s}$
	<i>T</i>	7.18	122
15	<i>L</i>	0.363	8.43
	<i>T</i>	0.0977	1.65

which is a much weaker scattering medium ( $\nu/\rho c_T^2 = -0.412$ ). The respective mean free times for each material defined as  $1/c\kappa$  are shown in Table II. The results from the solution of the URTE agree with intuition. The time for multiple scattering to dominate occurs between the longitudinal and shear mean free times. For lower frequencies this multiple scattering critical time is closer to the longitudinal mean-free time. At higher frequencies this critical time shifts toward the shear mean-free time. This result highlights the complications that arise as a result of the presence of two propagation modes with different wave speeds. It is also unclear which mean-free time is the more important of the two. One should keep in mind, though, that at times earlier than either mean-free time, the multiple scattering effects can be significantly greater than the singly scattered energy as Figs. 2 and 3 reveal. Thus examinations of mean-free times may not be enough for determining applicability of the single scattering approximation.

#### IV. DISCUSSION

Results have been presented for the multiply scattered solution in the time domain for ultrasonic scattering in a polycrystalline medium using ultrasonic radiative transfer theory. The multiply scattered solutions have very different behavior than the singly scattered solutions and contain additional microstructural information. It was also shown that multiple scattering effects may be significant at times on the order of a mean-free time or less.

One should keep in mind that the results presented here are for a plane wave at normal incidence. Experiments involving focused transducers have been modeled well using single scattering models for materials that scatter strongly. In these cases, multiple scattering effects are minimized by the finite beam width which allows very little of the multiply scattered energy to reenter the beam. However, as the beam focus is placed farther into the medium or as one examines later times, one would expect the multiple scattering effects to become more pronounced.

Boundary reflection effects, which are important in typical experiments performed in a water bath, have not been included thus far in this work. Inclusion of these effects into the URTE will be the subject of a later communication.

#### ACKNOWLEDGMENT

This work was sponsored by the National Science Foundation, Grant No. MSS-91-14360.

- <sup>1</sup>J. Saniie and N. M. Bilgutay, "Quantitative grain size evaluation using ultrasonic backscattered echoes," *J. Acoust. Soc. Am.* **80**, 1816–1824 (1986).
- <sup>2</sup>B. Fay, "Theoretical considerations of ultrasound backscatter" (in German) *Acustica* **28**, 354–357 (1973).
- <sup>3</sup>K. Goebbels, "Ultrasonics for microcrystalline structure examination," *Philos. Trans. R. Soc. London A* **320**, 161–169 (1986).
- <sup>4</sup>F. J. Margetan, T. A. Gray, and R. B. Thompson, "A technique for quantitatively measuring microstructurally induced ultrasonic noise," *Review of Progress in Quantitative NDE, 10*, edited by D. O. Thompson and D. E. Chimenti (Plenum, New York, 1991), pp. 1721–1728.
- <sup>5</sup>J. H. Rose, "Ultrasonic backscatter from microstructure," *Review of Progress in Quantitative NDE, 11*, edited by D. O. Thompson and D. E. Chimenti (Plenum, New York, 1992), pp. 1677–1684.
- <sup>6</sup>M. D. Russell and S. P. Neal, "Grain noise power spectrum estimation for weak scattering polycrystalline materials using experimentally estimated backscatter coefficients: normal incidence," *Ultrasonics* **32**, 163–171 (1994); and "Grain noise power spectrum estimation for weak scattering polycrystalline materials using experimentally estimated backscatter coefficients: oblique incidence," *Ultrasonics* **32**, 173–180 (1994).
- <sup>7</sup>W. P. Mason and H. J. McSkimm, "Attenuation and scattering of high frequency sound waves in metals and glasses," *J. Acoust. Soc. Am.* **19**, 464–473 (1947).
- <sup>8</sup>A. B. Bhatia, "Scattering of high-frequency sound waves in polycrystalline materials," *J. Acoust. Soc. Am.* **19**, 16–23 (1959).
- <sup>9</sup>E. P. Papadakis, "Scattering in polycrystalline media," *Meth. Exp. Phys.* **19**, 237–298 (1981).
- <sup>10</sup>D. W. Fitting and L. Adler, *Ultrasonic Spectral Analysis for Nondestructive Evaluation* (Plenum, New York, 1981).
- <sup>11</sup>A. Vary, "Ultrasonic measurement of material properties," *Research Techniques in Nondestructive Testing V,IV*, edited by R. S. Sharpe (Academic, New York, 1980), pp. 159–204.
- <sup>12</sup>C. B. Guo, P. Holler, and K. Goebbels, "Scattering of ultrasonic waves in anisotropic polycrystalline metals," *Acustica* **59**, 112–120 (1985).
- <sup>13</sup>R. L. Weaver, "Diffusivity of ultrasound in polycrystals," *J. Mech. Phys. Solids* **38**, 55–86 (1990).
- <sup>14</sup>J. A. Turner and R. L. Weaver, "Radiative transfer of ultrasound," TAM Report No. 725, University of Illinois, September, 1993; J. A. Turner and R. L. Weaver, "Radiative transfer of ultrasound," *J. Acoust. Soc. Am.* **96**, 3654–3674 (1994).
- <sup>15</sup>J. A. Turner and R. L. Weaver, "Radiative transfer and multiple scattering of diffuse ultrasound in polycrystalline media," TAM Report No. 738, University of Illinois, November, 1993; J. A. Turner and R. L. Weaver, "Radiative transfer and multiple scattering of diffuse ultrasound in polycrystalline media," *J. Acoust. Soc. Am.* **96**, 3675–3683 (1994).
- <sup>16</sup>S. Chandrasekhar, *Radiative Transfer* (Dover, New York, 1960).
- <sup>17</sup>V. V. Sobolev, *A Treatise on Radiative Transfer* (Van Nostrand, Englewood Cliffs, NJ, 1963).
- <sup>18</sup>A. Ishimaru, *Wave Propagation and Scattering in Random Media* (Academic, New York, 1978), Vol. 1.
- <sup>19</sup>L. Tsang, J. A. Kong, and R. T. Shin, *Theory of Microwave Remote Sensing* (Wiley, New York, 1985).
- <sup>20</sup>R. L. Weaver, "On diffuse waves in solid media," *J. Acoust. Soc. Am.* **71**, 1608–1609 (1982).
- <sup>21</sup>J. A. Turner, "Radiative transfer of ultrasound," Ph.D. thesis, Department of Theoretical and Applied Mechanics, University of Illinois (1994).